Low seismic velocity layers in the Earth's crust beneath Eastern Siberia (Russia) and Central Mongolia: receiver function data and their possible geological implication

Yu.A. Zorin [a,*], V.V. Mordvinova [a], E.Kh. Turutanov [a], B.G. Belichenko [a], A.A. Artemyev [a], G.L. Kosarev [b], S.S. Gao [c]

[a] *Institute of the Earth's Crust, Siberian Division of Russian Academy of Sciences, 128 Lermontov str., 664033 Irkutsk, Russia*
[b] *United Institute of Physics of the Earth, Russian Academy of Sciences, 10 Bolshaya Gruzinskaya str., 123810 Moscow, Russia*
[c] *Department of Geology, Kansas State University, 207 Thompson Hall, Manhattan, KS 66506-3201, USA*

Abstract

Analysis of teleseismic receiver functions at digital stations along the Bratsk–Irkutsk–Ulanbaatar–Undurshil profile suggests that low-velocity layers in the Earth's crust exist not only beneath the Baikal rift zone, where such a layer was found earlier by Deep Seismic Sounding (DSS), but also beneath Early Paleozoic Sayan–Baikal, Paleozoic Mongolian, Early Mesozoic Mongolia–Okhotsk fold areas, and beneath the Siberian platform. The reliability of detection of the low-velocity layers by receiver function analysis has been checked by numerical modeling. The results of this modeling demonstrate that receiver functions can reveal the low-velocity layers in the crust if the initial model (starting approximation) is close to real velocity distribution, and if the model medium is divided into thin layers. Averaged DSS velocity model without low-velocity layers was used as starting approximation for the inversion of observed receiver functions. The low-velocity layers are interpreted to reflect inhomogeneities of the Earth's crust formed during its evolution. Most of these layers are presumed to correspond to thick mylonite zones related to large pre-Cenozoic thrusts. The mylonites possess a great seismic anisotropy caused by the mineral orientation formed by the ductile flow in large thrust zones. They can result in low-velocity layers only for seismic waves whose rays are oriented perpendicular to the mylonite foliation, i.e., in the direction of the minimum velocity; the velocities along the foliation direction can be rather high. Therefore, the low-angle mylonite zones can be distinguished by the receiver function method, which uses the waves from the teleseismic events with nearly vertically oriented rays. The suggestion that the low-velocity layers mark low-angle thrusts is in agreement with gravity and geological data. The amount of overthrusting is estimated to be as large as several hundred kilometers. Multichannel seismic profiling can be used to verify the existence and the deep geometry of the presumed thrusts.
© 2002 Elsevier Science B.V. All rights reserved.

Keywords: Low-velocity layers; Mylonites; Seismic anisotropy; Thrusts

---

* Corresponding author. Fax: +7-3952-462900.
E-mail address: zorin@crust.irk.ru (Yu.A. Zorin).

1. Introduction

A low-velocity layer was first identified in the Earth's crust of Eastern Siberia by Deep Seismic Sounding (DSS) in the area of the Baikal rift zone based on the offset of the time–distance dependence for the refracted waves at an epicentral distance of 100–170 km (Krylov et al., 1981). The depth to the upper boundary of this layer varies from 8 to 16 km, its thickness is estimated to be 5 km, and the P-velocity decrease relative to the surrounding medium is 0.2–0.3 km/s. Such a layer has not been found beneath the Siberian platform. Although this layer was also identified in the western Trans-Baikal region—near Khilok, which is not part of the Baikal rift zone—it was considered as a characteristic fea-

ture of the Cenozoic rift zone (Krylov et al., 1981). This layer was suggested to correspond to a layer of high electrical conductivity, found by magnetotelluric soundings at approximately the same depth (Popov, 1989), and was interpreted as a zone saturated by mineral water as a result of rock dehydration due to crustal heating during Cenozoic rifting (Krylov et al., 1981; Popov, 1989).

More detailed studies using refracted waves have shown that the low-velocity layer in the crust of the Baikal rift zone is not continuous but a fragmentary feature (Pusyrev, 1993). A study across the SW boundary fault of the Upper Angara Rift Basin using vertically reflected waves found that a set of interrupted reflectors dips northeastward at an angle of about 35–40° to a depth of 15 km, and then becomes
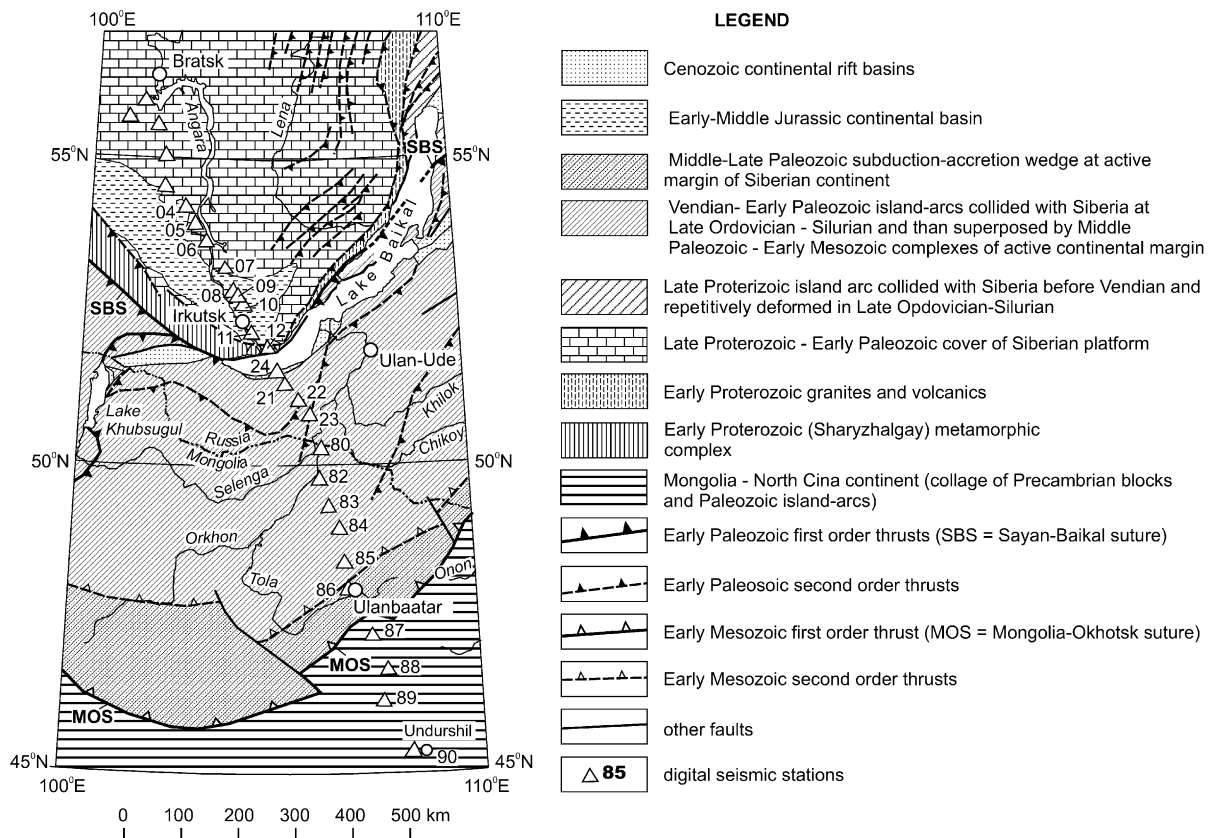

Fig. 1. Location of the digital seismic stations on the Bratsk–Irkutsk–Ulanbaatar–Undurshil profile and tectonic sketch map of Eastern Siberia and Central Mongolia. The stations are shown by the triangles; the stations, the records of which are used in this study, are additionally marked by the numbers. Tectonic sketch map is compiled from Sizykh and Lobanov (1994), Zorin et al. (1994) and Zorin (1999). Note that the thrusts are widespread in this region. The Early Paleozoic thrusts possess northwestern vergence, and the Early Mesozoic thrusts have southeastern vergence.

very low-angle, trending into the sub-horizontal low-velocity layer. It was suggested that the low-velocity layer beneath the Upper Angara Basin corresponds to the tectonite zones related to a large-scale, low-angle fault (Pusyrev, 1993).

The low-velocity layer was also found in the eastern Trans-Baikal region, in the southern part of the Chita Region, at depths ranging from 8 to 14 km (Argutina et al., 1974) using converted waves. Because the application of converted waves was not popular at that time, anomalous converted waves, which could come from the top of a low-velocity layer, were not geologically interpreted. Much later, an attempt was made to interpret this interface as the bottom of the Onon allochthon composed of Paleozoic metamorphic rocks and overthrust Triassic and Jurassic strata (Zorin et al., 1995).

So, the generally accepted view that a low-velocity crustal layer is a feature of only the Baikal rift zone and reflects its thermal and fluid regime seems to be doubtful. These layers more likely reflect low-angle fault zones, movements along which cause tectonic layering of the Earth's crust. According to the geological data, there are many pre-Cenozoic thrusts in the study region (Fig. 1). Geodynamical analysis shows that some of these thrusts are of crustal-scale (Zorin, 1999; Zorin et al., 2001). The zones of such thrusts can correspond to the low-velocity seismic layers. This paper presents the new data, obtained from receiver function analysis, on the low-velocity layers in the crust of the Siberian platform, the Sayan–Baikal Early Paleozoic fold area (part of which is superposed by the Baikal rift zone), the Mongolia–Okhotsk Mesozoic fold belt, and the Mongolian Paleozoids.

2. Seismic data

The teleseismic dataset that we used in this study was recorded by digital seismic (Reftek) stations deployed along the Bratsk–Irkutsk–Ulanbaatar–Undurshil profile in a 4-month period in 1992 as a part of the PASSCAL (Program for the Array Seismic Study of Continental Lithosphere) experiment (Gao et al., 1994). This profile traverses the major tectonic units of Eastern Siberia (Russia) and Central Mongolia (Fig. 1). All the 28 profile stations were equipped

with 1 Hz three-component L4C seismometers which recorded ground velocity.

We selected the records of teleseismic events with body wave magnitudes 5.0 or larger in the epicentral distance range from 40° to 80°. The back azimuths for most of the events range from 120° to 200° (Fig. 2). For each station, we used records from 8 to 12 events with relatively simple waveforms and sharp first arrivals (Fig. 3). Twenty-three stations marked by numbers in Fig. 1 were found to have enough high-quality records to be used for receiver function analysis.

3. Seismic data processing and inversion

3.1. Basic principles

The receiver function method is described in many works (e.g., Langston, 1979; Vinnik et al., 1988; Ammon et al., 1990; Kind et al., 1999). The method uses P-to-S converted waves at crustal and mantle interfaces beneath the seismic stations. These waves (transmitted and reflected) must be isolated from the coda of the teleseismic P-wave. For this, three-component original records are rotated into the ray coordinate system L, Q and T. The L contains mainly P-energy, Q mainly SV-energy and T mainly SH-energy. The Q-component contains the information on P-to-SV converted waves. The seismograms are source-equalized by deconvolution of the Q-component with L-component to obtain receiver functions (Petersen and Vinnik, 1991; Kind et al., 1999). Receiver functions from several events are summed to improve the signal-to-noise ratio.

Computation of the complete theoretical plane–wave seismograms used in the inversion process were made using the Thompson–Haskell method (Haskell, 1962). The search for the best-fitting model was based on the general method of solving ill-posed inverse problems (Tikhonov and Arsenin, 1979). We divided the model medium into thin layers with fixed thickness (vertical step of model) and gave each layer a starting velocity (see below). We then determined S-velocity in those layers using above inversion procedures described in detail in Vinnik et al. (1988), Petersen and Vinnik (1991), and Kind et al. (1999).
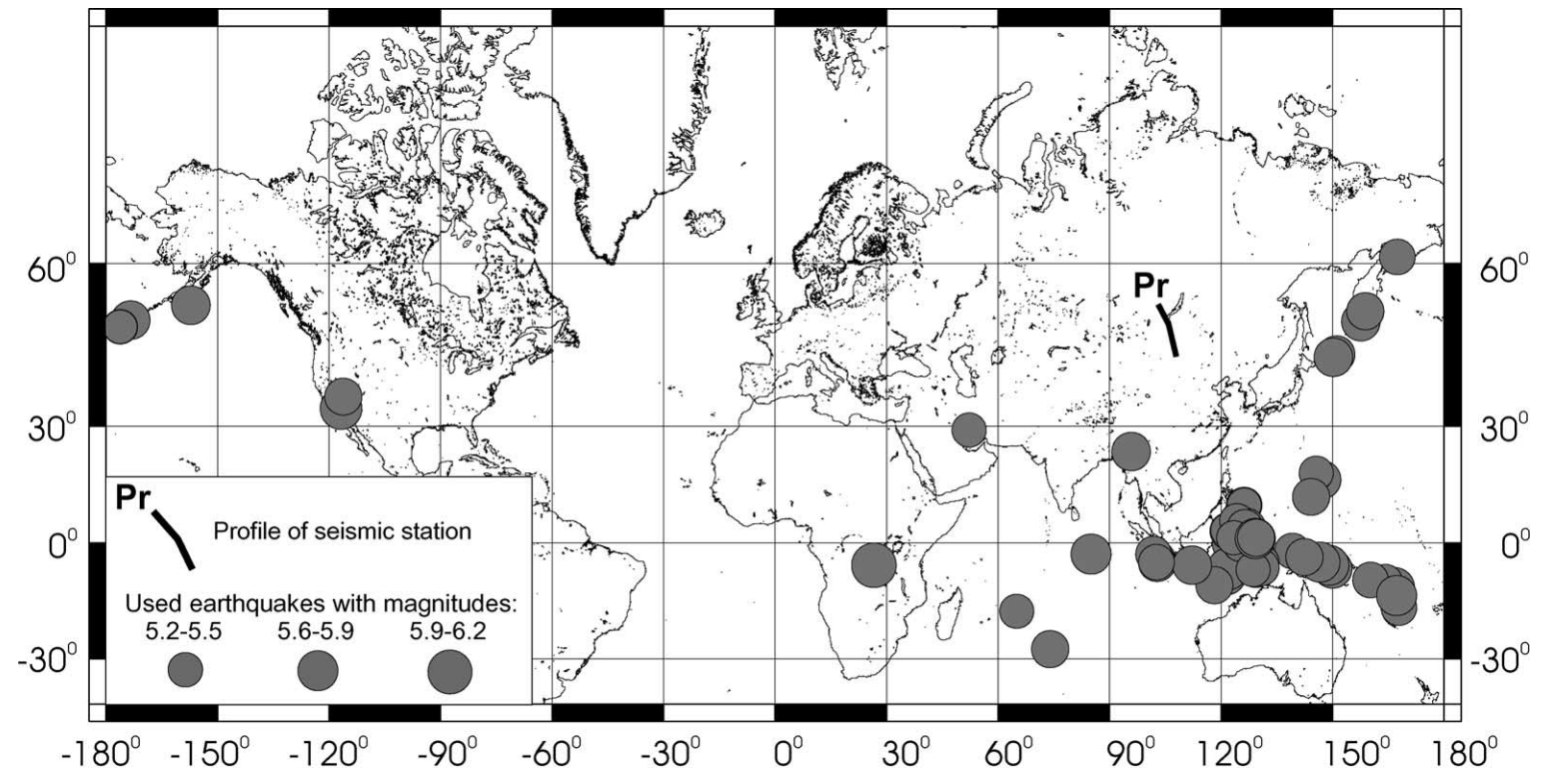
Fig. 2. Location of the seismic profile and used earthquakes.

ST 89

Earthquake 215: 08.02.92; T_0=12.03.20.2; φ=-7.12^0; λ=121.72^0;
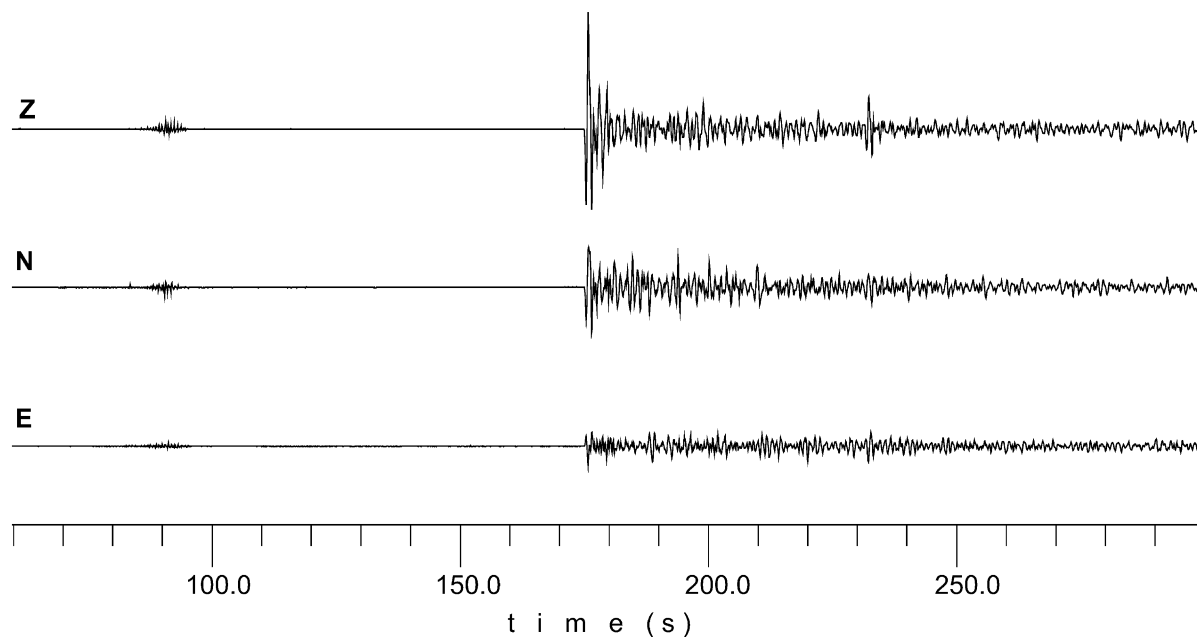M=6.2; H=483 km; D=56.33^0; Az$_{back}$=162.3^0

Fig. 3. Example of used seismic records (earthquake 215: 08. 02. 92) at the station 89 (see Fig. 1). T_o = time of earthquake; φ = latitude; λ = longitude; M = magnitude; H = depth of hypocenter; D = epicentral distance; Az$_{back}$ = back azimuth.

The receiver function method used here deals with one-dimensional models. However, for each station, we obtain information about a limited area where converted and multiply reflected waves are formed. The horizontal dimension of this area is approximately equal to the depth of the boundary (Kurita, 1947; Mordvinova, 1988; Mordvinova et al., 1995). We consider here only interfaces with depths of no more than 55 km. The distances between the stations are 30–70 km. If the layers and interfaces are correlated between stations, we can obtain a two-dimensional and, in the case of a 2D seismic array, even a three-dimensional structure of the crust.

As most of the events that we used were from the southeast (see Fig. 2), the resulting velocity structure for a given station is shifted southeastward. At teleseismic distances, such displacement (so-called "seismic stretch") can reach up to 20 km at 40-km depth. Displacement decreases upward pro rata with depth.

The seismic data were band-pass filtered in the frequency band from 0.2 to 0.9 Hz, on basis of the frequency response of the L4C sensors and the frequency compositions of teleseismic P-waves and noise (Fig. 4). The total length of the used seismograms was 100 s, including 40 s before the first arrival. Theoretical waveforms were computed with a V_P/V_S velocity ratio of 1.73. The density was determined according to the Birch's law (Birch, 1961). Inversion routine uses the first 25 s of the synthetic receiver functions to compare with that of the observed ones.

3.2. Synthetic testing of the resolving power of the inversion procedure

3.2.1. General approach to modeling

We next created synthetic seismograms for crustal models with one, two and three low-velocity layers to
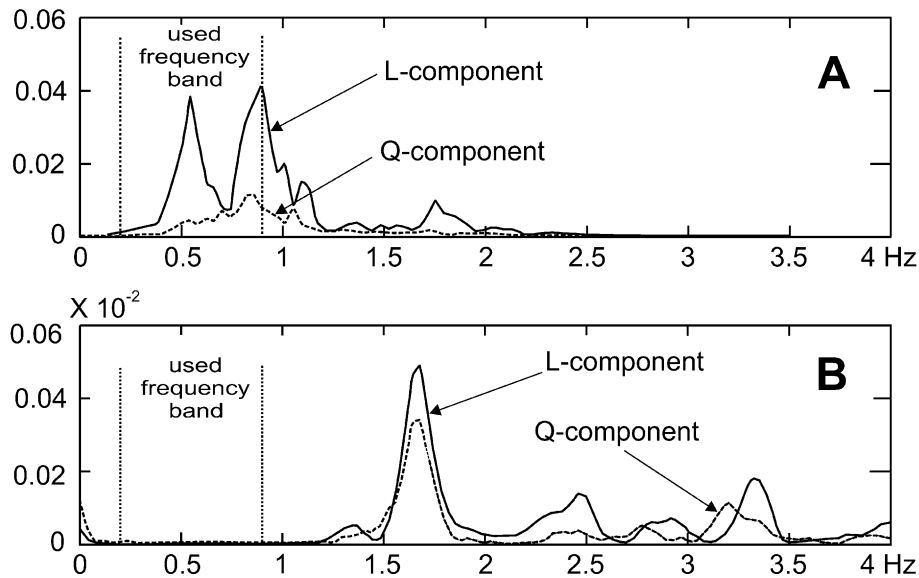
Fig. 4. Power spectral densities of seismic record (see Fig. 3) rotated into the ray coordinate system L, Q and T. (A) Spectral densities calculated for all time interval shown in Fig. 3; (B) spectral densities of noise calculated for time interval from 0 to 170 s before arrival of the teleseismic signal. Note that vertical scale of (A) exceeds that of (B) in two orders.

test the resolution of the receiver function inversion procedure. Results for the models with two low-velocity layers are shown in Figs. 5 and 6. Major conclusion from a model with two low-velocity layers is similar to those from models with one or three low-velocity layers.

To perform the testing, we first created a model ("the primary models") with low-velocity layers inserted into averaged velocity–depth model, which was constructed from DSS for the Sayan–Baikal mountain region (Pusyrev, 1993). The thicknesses of the low-velocity layers were 4 and 6 km (see Section 5.1). We calculated synthetic SV-waveforms using the primary models and the real stacked P-signal from station 4. To take into account the SV-waveform distortions after conversion, we introduced in these waveforms the random noise. The peak amplitude of the noise is 15% of that of SV-oscillations. The

synthetic seismograms (together with noise) were filtered in the 0.2–0.9 Hz band.

We next inverted the synthetic data to produce velocity models ("secondary models"). In most cases, the starting model for the inversion was the same averaged DSS velocity–depth model (Pusyrev, 1993) without low-velocity layers. This starting model was modified only for testing dependence of resolving power on assumed value of a mean velocity (see Section 3.2.4).

3.2.2. Resolution and vertical step in the models

To demonstrate dependence of the resolving power of the inversion procedure on the size of vertical steps, we use a primary model with the S-wave velocity decrease of 0.3 km/s in the low-velocity layers relative to surrounding medium. This value is close to the maximum velocity decrease obtained from the inver-

Fig. 5. Resolution of the receiver function inversion for a model of the crust with two low-velocity layers depending on vertical step in secondary models. The seismic cross-sections are shown in the left parts of the boxes and related waveforms are shown in the right parts of the boxes. (A) Depths of layer boundaries in the secondary model coincide with those in the primary model, vertical steps for both models are 2 km; (B) layer boundaries in the secondary model are 1 km shifted relatively those in the primary model, the vertical steps for both models are 2 km; (C) layer boundaries in the secondary model are 0.5 km shifted relatively those in the primary model, the vertical steps for the secondary model are 1 km.
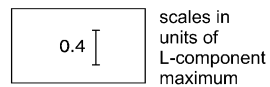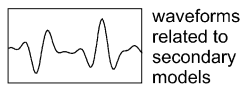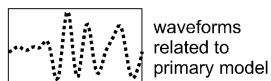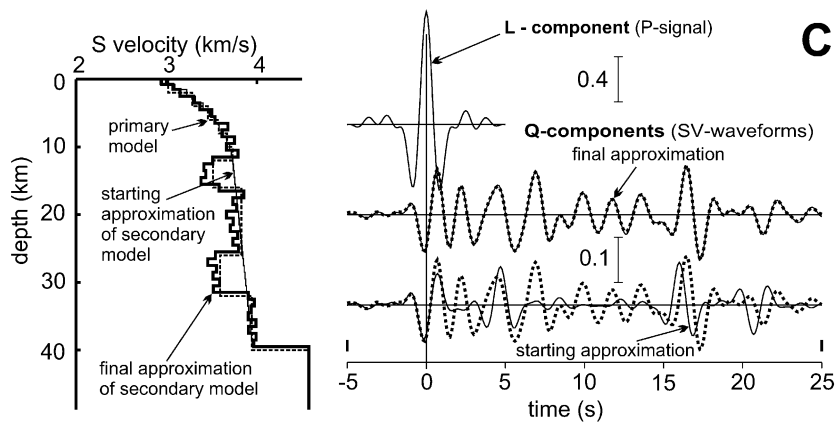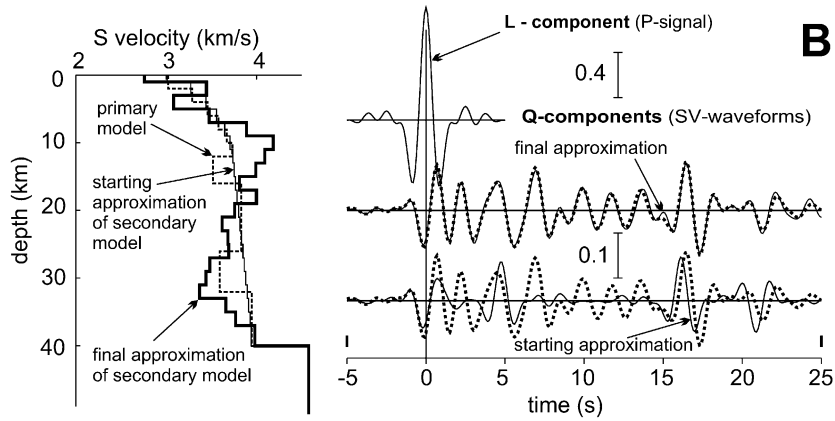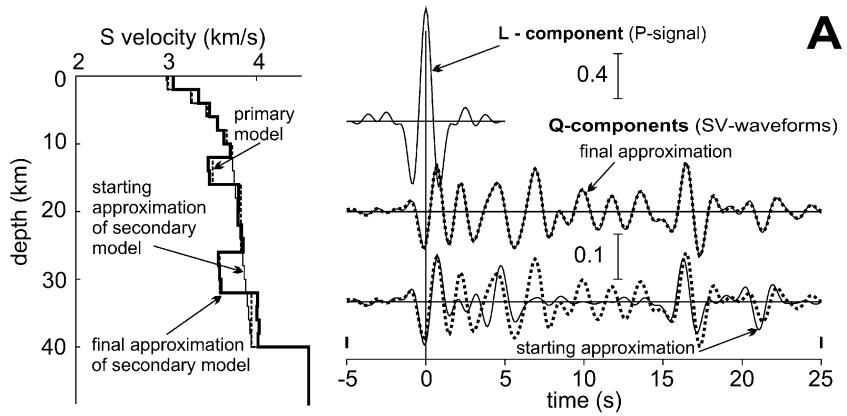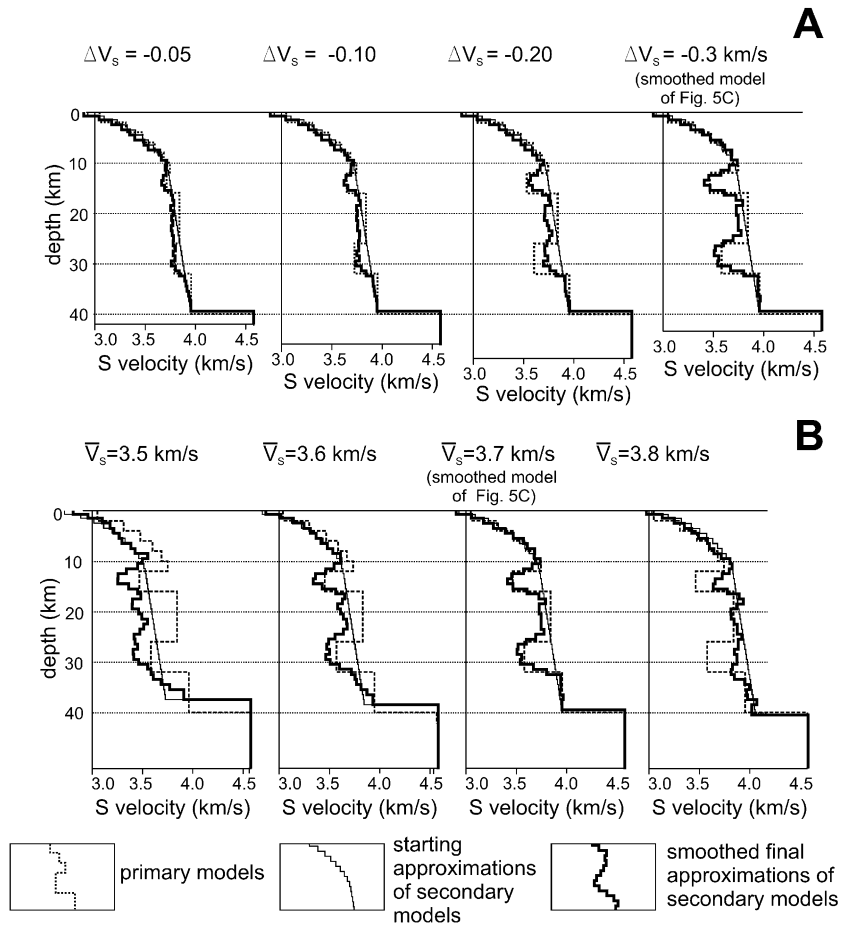
Fig. 6. Resolution of the receiver function inversion for a model of the crust with two low-velocity layers depending on relative S-wave velocity contrast (ΔV) in the low-velocity layers (A) and on mean crustal velocity (V_S) in the starting approximation (B).

sion of observed receiver functions (see Section 4). When layer boundaries have the same depths in both primary and secondary models with a 2-km vertical step, the primary model is well recovered by the inversion (Fig. 5A). The primary model is recovered completely when noise-free data are used (result is not shown). Naturally, in real conditions, the depths of the layer boundary taken a priori in the model are likely not to coincide with depths of conversion interfaces in the crust. However, even being artificial, such models are in a certain sense useful. They demonstrate that the primary models with low-velocity layers can be recovered even though the arrivals of the converted waves, associated with the boundaries of the low-velocity layers, cannot be distinguished on SV-wave-

forms because of mutual superposition of the phases (Fig. 5A, right side).

Recovering of the primary model worsens dramatically when the boundary depths of the layers in the starting approximation of the secondary model are displaced by 1 km relative to their position in the primary model with a vertical step of 2 km (Fig. 5B). Such disagreement between primary and secondary models is rather natural because the inversion program tries to correct rather significant (about 0.3 s) phase shifts associated with the shift of the interface depths.

An effective way to reduce such phase shift is to decrease the thickness of layers in the secondary models. We tested the secondary models with vertical

step of 1 km and with displacement of 0.5 km between boundary depths of primary and secondary models. It turned out that the primary models are well recovered, although there are some additional velocity oscillations (Fig. 5C). The oscillations can be suppressed by smoothing the resulting secondary model using running window of a rather small size. All of the secondary models described below were constructed with 1-km step using 0.5-km displacement of boundaries and with subsequent smoothing of the S-wave velocity with a three-step running window.

3.2.3. Resolution and S-wave velocity decrease

Taking into account the results of real data inversion (see Section 4), we tested the resolution of the receiver functions for detecting the low-velocity layers with different S-wave velocity decreases. For this test, we used the same conditions as in the model shown in Fig. 5C, but varied the velocity decrease in primary models from 0.05 to 0.3 km/s at the upper boundary of the low-velocity layers. The target low-velocity layers are detected rather reliably for all of the models but some complications are apparent when the velocity contrasts are low (Fig. 6A). For example, an additional false, weakly expressed low-velocity layer appears in the central part of the crustal model when the velocity contrast is −0.2 km/s. Further reduction of velocity contrast to −0.1 and −0.05 km/s results in loss of information on the position of upper boundary of the deeper low-velocity layer. In this situation, only the midpoint of this low-velocity layer can be detected relative to the starting velocity−depth model (Fig. 6A). All of these complications are connected with additional noise as well as with superposition of the phases from different conversion boundaries.

3.2.4. Resolution and starting velocity−depth models

In principle, the receiver function inversion is non-unique (Ammon et al., 1990). To minimize such non-uniqueness in a situation with fixed vertical steps, it is necessary to use the starting velocity model that is close to a real velocity structure. The dependence of inversion results on mean velocity variations in the starting approximation is demonstrated for the primary model with relative velocity decrease of 0.3 km/s. To construct the secondary models, we used the starting approximations with mean S-wave crustal

velocities of 3.5, 3.6, 3.7, and 3.8 km/s keeping the same gradient of the velocity increase with depth that was obtained by DSS (Fig. 6B). A change of the mean crustal velocity leads to a virtual proportional change in the vertical scale of the secondary model. Consistent with this, the Moho depth in above starting models was proportionally changed while keeping the 1-km vertical step.

The modeled low-velocity layers are detected rather well taking into account some shifts caused by virtual change of vertical scale. However, fixed vertical step and introduced additional noise result in some distortion in the final model. Specifically, a false, weakly expressed low-velocity layer appears between modeled layers when the mean crustal velocity deviates from its real value (Fig. 6B).

3.2.5. Some implications of the modeling

To detect low-velocity layers in the Earth's crust, the vertical step in the interpretative model has to be small enough: it must be at least three times less than thickness of the target layer. The velocity distribution in the starting model has to be reasonably close to the real crustal seismic structure. It should be noted that sufficient reproduction of the existing low-velocity layer (even with relative velocity contrast as small as −0.05 km/s) does not exclude the appearance of artifacts in the final results of the modeling. These artifacts can become apparent as velocity distortion in the target layers and their vicinity and/or as appearance of false, weakly expressed low-velocity layers.

3.3. Characteristics the models used for inversion of observed receiver functions

Based on the modeling results, we took the thickness of layers (vertical step) to be 1 km for the most part of the crust in the receiver function inversion. A step of 0.5 km was used for the uppermost part of the crust (depths from 0 to 4−5 km), where the velocities are the most variable. A 1-km step was also used for upper 4−6 km of the mantle, and a 5-km step was used below this depth to 75 km, beneath which the mantle was considered as a homogenous half-space. The final models were smoothed using a three-step running window (Fig. 7).

The starting S-wave velocity model of the crust was constructed using the averaged DSS velocity−

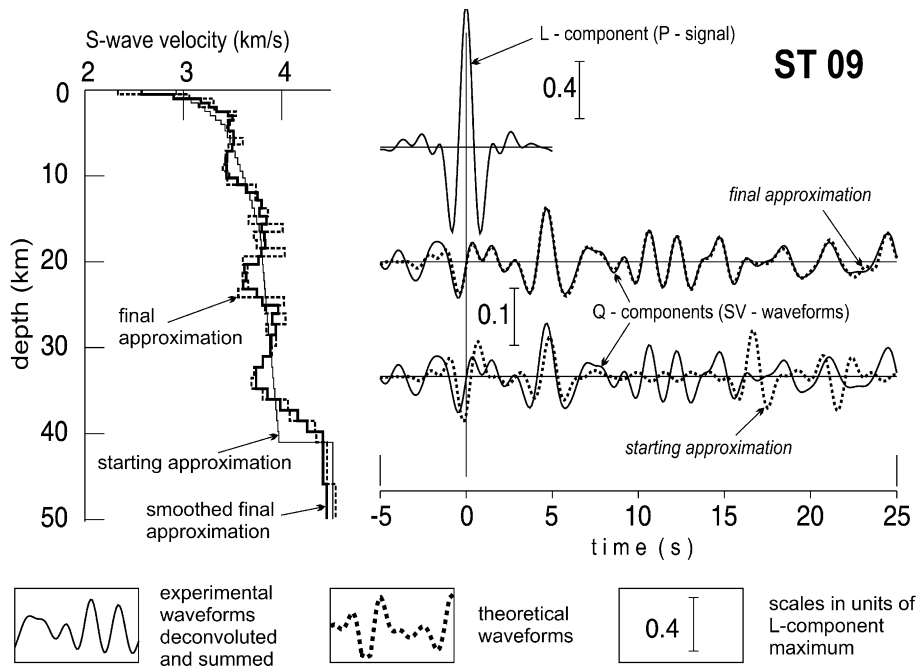Fig. 7. Example of the receiver function inversion (station 09). The seismic cross-sections are shown in the left parts of the box and waveforms are shown in the right parts of the box. Vertical bars above time scale limit the interval of waveforms used for inversion.
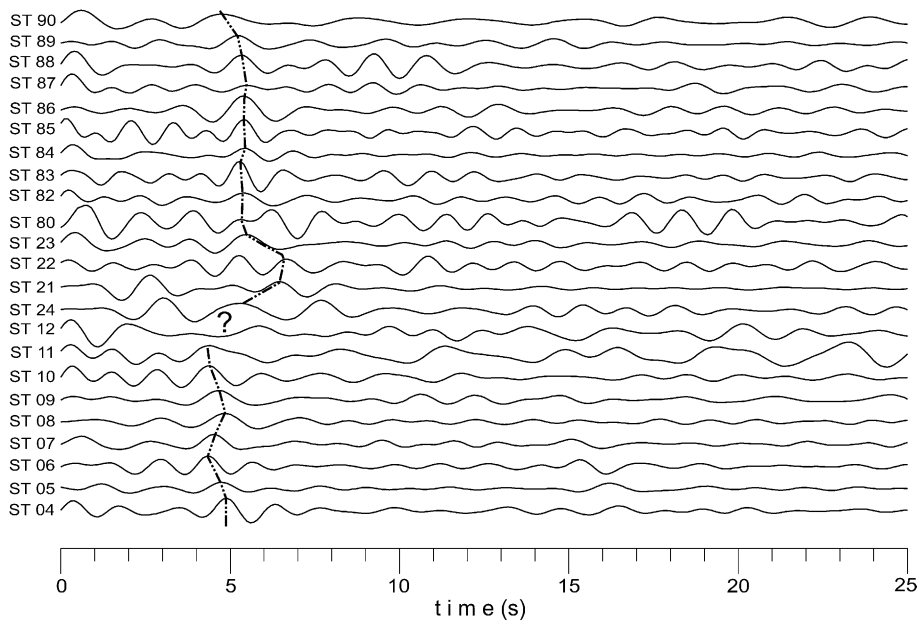

Fig. 8. Deconvoluted and stacked SV-waveforms for the stations of profile. Dashed line shows correlation of the maxima related to conversion at the Moho.

depth model for the Sayan–Baikal mountain region without the low-velocity layers (Fig. 7). This model was modified for each station by changing the vertical scale of the velocity-versus-depth curve (while keeping the size of the vertical steps), in accordance with the crustal thickness estimated from the maximum related to the Moho in SV-waveforms (Fig. 8). The starting S-wave velocity model was constructed using P-wave velocities (Pusyrev, 1993) divided by 1.73, as P-wave velocities in the crust are usually better determined than S-wave velocities. Since the variations of the mean crustal P-wave velocity estimated by DSS in different regions of Eastern Siberia do not exceed 0.2 km/s (Pusyrev, 1993), we assume that the use of the averaged DSS velocities as the starting models is reasonable for the inversion of receiver functions. Thus, our task is reduced to a rather simple one: detecting low-velocity layers based on a well-determined velocity model from DSS.

4. Results of receiver function inversion

P-to-S conversions from the Moho can be recognized on most of the stations from stacked receiver functions (Fig. 8). The amplitude of the conversions is weak in the Baikal rift zone (stations 12, 24, 21, 22, and 23) where an intermediate zone between crust and mantle might exist (Pusyrev, 1993).

In the final results of inversion, the Moho corresponds to an abrupt S-wave velocity increase (Fig. 9). The crustal thickness varies from 37 to 40 km beneath the Siberian platform (stations 04–11). It is about 34 km beneath the station 12, which is on the NW side of the Lake Baikal and reflects the crustal structure beneath the lake due to seismic stretch (see Section 3.1). The crustal thickness increases abruptly up to 51 km beneath station 24, which is on southeastern side of the lake and reflects the crustal structure beneath the Khamar Daban ridge due to seismic stretch. The maximum crustal thickness (55 km) is found beneath the station 21 (axial part of the Khamar Daban ridge). The thickness gradually decreases to 45 km beneath the stations 83 and 84. Beneath the rest of the southeastern part of the profile the Moho depths vary from 44 to 48 km. Generally, the crust is thicker beneath the fold areas of Siberia and Mongolia than that beneath the Siberian platform. The aforementioned values of

the crustal thickness are in agreement with the DSS data for Russian part of the profile (Krylov et al., 1981; Pusyrev, 1993).

The low-velocity layers are identified in the Earth's crust as velocity minima on smoothed velocity models beneath almost all the stations (Fig. 9). The S-wave velocity decrease in the low-velocity layers relative to surrounding medium varies from 0.1 to 0.4 km/s. We consider only the low-velocity layers with a thickness of three or more vertical model steps. These layers can be correlated from one station to another without difficulty, if their depths are not very different beneath neighboring stations. If the layer is inclined, it can be correlated taking into account benchmark boundaries (Earth's surface, Moho, sub-horizontal layers), the presence of an uppermost vacant (not occupied by earlier distinguished layers) velocity minimum beneath the neighboring station, and the general trend of the layer dip discovered from several stations. Moreover, geological and gravity data were used to correlate certain low-velocity layers, which may correspond to large thrusts (see below). The recognition of low-velocity layers was made in sequence from top to bottom.

To show layer correlation visually in Fig. 9, we have used S-waves velocity minima, but not the projections of these minima onto the vertical axes. Only the midpoints of the low-velocity layers are connected for the most of the layers. Boundaries are given only for certain layers, the thickness of which is used for further geological interpretation. Most of the layers are numbered in Roman numerals for ease of further reference (Fig. 9).

A low-velocity layer is identified beneath practically all of the stations in the uppermost part of the crust. The thickness of this layer is about 1–1.5 km within the fold areas. Its thickness increases to 2–3 km within the Siberian platform (stations 04–11). Only platform part of the layer is displayed and numbered in Fig. 9 (layer I). The reason for separation of this part of the layer is the existence of a thick sedimentary cover only in this section of the profile (see Fig. 1).

Layer II is well expressed beneath the Sayan–Baikal Early Paleozoic fold area, northwestern part of which is superposed by the Cenozoic Baikal rift zone. The depth of upper boundary of the layer ranges from 3 to 4 km, and that of the lower boundary ranges
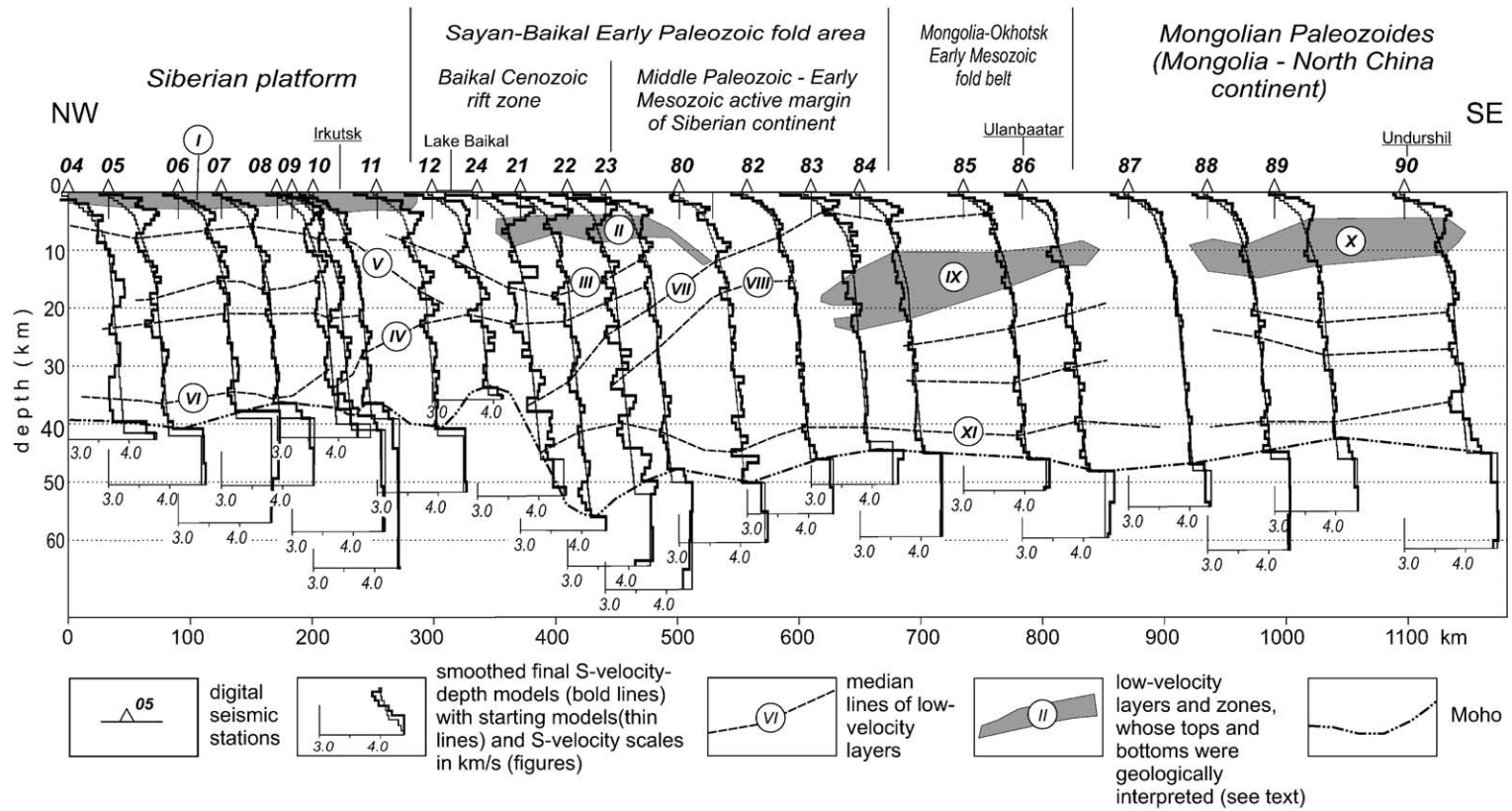
Fig. 9. Seismic model of the crust structure along the profile.

from 5 to 8 km (Fig. 9, stations 24, 21, 22, 23, and 80). We did not extend this layer into the Siberian platform (for example, in position of layer III beneath the stations 12–11 and then in position of layer V beneath the stations 10-04) since these layers bound from below the uppermost parts of the crust whose ages and compositions are quite different within the platform and within the fold areas.

Beneath stations 11, 12, 24, 21, 22, and 23, there is low-velocity layer III, with the depth of its roof varying from 8 to 18 km and with the thickness varying from 3 to 6 km (Fig. 9). Judging by its depth and thickness, we presume that this layer corresponds to a low-velocity layer distinguished by the DSS beneath the Baikal rift zone (Krylov et al., 1981). We have made a decision to extend this layer to uppermost vacant velocity minima beneath the stations 12 and 11, i.e., only beneath the narrow marginal part of the Siberian platform which forms the northwestern rift shoulder.

The central line of layer IV is seen at the depths range from 16 to 22 km beneath stations 23, 22, 21, 24, and 12. Layer IV probably continues beneath stations 11, 10, 09, 08, and 07, dipping northwestward to the Moho (Fig. 9). The layer cuts off the oppositely dipping layer V beneath the stations 04–11. The correlation of layer V between stations 04 and 10 is evident (Fig. 9). The extension of this layer beneath station 11 with an increased dip angle is determined by the presence of the uppermost vacant velocity minima as well as by our intention to limit a thickened part of the body composed by the Sharyzalgay metamorphic complex which produces a positive gravity anomaly (see below).

Two low-velocity layers in this part of the profile (unnumbered) are found at the depths of 15–19 km (stations 05–08) and at depths of 21–23 km (stations 04–10). A similar layer is identified near the Moho (layer VI beneath the stations 04–06).

Layer VII is observed beneath the stations 85, 84, and 83 at a depth of 3–4 km and dips to 8 km beneath the stations 82 and to 13 km beneath the station 80. Given that this layer dips northwestward, that coincides with the dip direction of Mesozoic large-scale thrust in Ulanbaatar region (Zorin, 1999), and taking into account velocity minima being not occupied by previously identified layers, we have correlated the layer VII to station 24, where the

Moho depth changes abruptly (Fig. 9). Layer VIII is found beneath the stations 22, 23, 80, and 82, and is parallel to the layer VII.

The rather thick low-velocity zones IX and X are found in the upper part of the crust beneath stations 83–86 and 88–90 (Fig. 9). Thin low-velocity layers (unnumbered) are found at depths of 20–22 and 30–33 km beneath stations 83–86 and also at depths of about 20 and 25 km beneath stations 88–90. The interrupted low-velocity layer XI is traced near the Moho from the station 24 to the station 90 (Fig. 9).

5. Possible geological implication of the low-velocity layers

5.1. On the nature of the low-velocity layers

Low-velocity layers are found by receiver function analysis in all the tectonic provinces traversed by the profile at different depths. Although the dip angles of the layers do not exceed 10–15°, some of the layers (IV, VII, and VIII) cut through different depth levels of the crust. Such crustal features cannot be connected with dehydration of the rocks (see Section 1), which can occur under certain P–T conditions changing with depth. We suggest that all of the low-velocity layers, as well as the high-velocity layers between them, reflect the inhomogeneity of the Earth's crust caused by different (mostly tectonic) geological processes that have taken place in various periods of crustal evolution.

The low-velocity layers might correspond to either sedimentary strata overthrust by sheets of crystalline rocks, or thick zones of tectonically destroyed rocks (fracture and cataclastic zones) associated with large-scale thrusts and listric faults. The origin of low-velocity layers and zones can be caused not only by tectonic processes, but also by magmatic ones. In particular, granitic bodies hosted by metamorphic rocks possess relatively low velocities.

All the aforementioned low-velocity layers and zones should be revealed both by DSS and receiver functions. In principle, the first method possesses a higher resolution than the second one, mostly due to the smaller wavelength. However, using receiver functions, we were able to find 3–4 low-velocity layers in all the tectonic provinces along the profile,

while the DSS detected only one such layer, and only in the Baikal rift zone.

We suggest that the difference in results between receiver functions and DSS can be explained by the following. Tectonic destruction of the rocks by fracturing and cataclasis generally takes place in the uppermost crust during the evolution of the thrusts and listric faults. Brittle deformation along the walls of the low-angle faults transforms, at some depth, into ductile flow with the formation of thick zones of mylonites. As a result of denudation (sometimes tectonic), some parts of these zones are exposed. The thickness of the mylonite zones associated with the faults along the boundaries of the Siberian platform varies from 2 to 8 km, but is usually 4–6 km (Zamaraev, 1967), which is comparable to the thickness (3–6 km) of the low-velocity layers (Fig. 9). The mylonitization at great depths, without open cracks or a significant reduction in density, does not lead to a reduction in seismic velocity. However, the re-orientation of minerals (mostly amphiboles and micas) in the zone of ductile flow results in seismic anisotropy: the velocities in the direction orthogonal to the mylonite foliation are less than those in the plane of the structures. Laboratory measurements of seismic velocities in rock samples (Christensen, 1965) and field experiments (Rabbel, 1994) proved that the anisotropy can be more than 10% in metamorphic rocks with clearly expressed planar structures. Therefore, receiver functions using seismic waves with subvertical rays identify more low-angle low-velocity layers than DSS using refracted and wide-angle reflected waves, whose rays deviate significantly from the vertical. Thus, the receiver function method is an acceptable tool for revealing the mylonite zones associated with the low-angle thrusts and the deep parts of listric faults. Probably only thick, water-saturated, sub-horizontal tectonite zones, renewed by recent movements, can be detected by the DSS method.

5.2. Comparison of seismic and gravity models

We used gravity data to verify the conclusion that most of the low-velocity layers correspond to large-scale thrusts that separate different rock complexes. Decompensative gravity anomalies (Zorin et al., 1985; Cordell et al., 1991) are used to construct a two-dimensional gravity model of the upper part of the

Earth's crust along the seismic profile (Fig. 10). The calculation of these anomalies is based on the assumption that large upper crustal density inhomogeneities as well as topographic masses are isostatically compensated. Isostatic reduction eliminates the gravity effects of topography and its compensation, but gravity effects of the upper crustal density inhomogeneities and their compensation remain. Eliminating influence of the last compensation by a special transformation of the isostatic anomalies, we can obtain the decompensative anomalies which are produced mainly by the density inhomogeneities in the upper 15–20 km of the crust (Zorin et al., 1985; Cordell et al., 1991).

The inversion of gravity anomalies was conducted using the semi-automatic Marquardt method (Cordell et al., 1992) that enables to determine the anomalous densities of geological bodies and/or the position of vertices of polygons, which represent vertical cross-sections of horizontal prisms used to model these bodies. Geological and seismic data were used as constraints on the inversion of gravity field. The nature of the anomalous bodies and the position of their exposed portions were determined from geological data (Zorin et al., 1994). The points determined by receiver functions and corresponding (as we suppose) to the attracting body boundaries were taken to be fixed, i.e., their positions were not changed during the inversion. We have chosen the fixed points on the top and on the bottom of the low seismic velocity layer when, according to the geological data, we could assume that this layer corresponds to a sedimentary rock unit overthrust by metamorphic rocks or to a granitic body. But in most cases, the boundaries of anomalous bodies are assumed to coincide with thrusts in crystalline rocks. In these situations, we have chosen the fixed boundary points of the attracting bodies as the midpoints of low-velocity layers, since the mylonitization takes place in both the hanging walls and footwalls of the thrusts. The fixed points are shown in Fig. 10, where "seismic stretch" has been taken into account. Results of multichannel seismic profiling (Hathcinson et al., 1992) were used to calculate the gravity anomaly from the lens of Cenozoic sediments in the Baikal rift.

Agreement between gravity and seismic models is demonstrated by the opportunity to adapt the calculated gravity anomalies to the observed ones under the assumption that the density discontinuities coincide
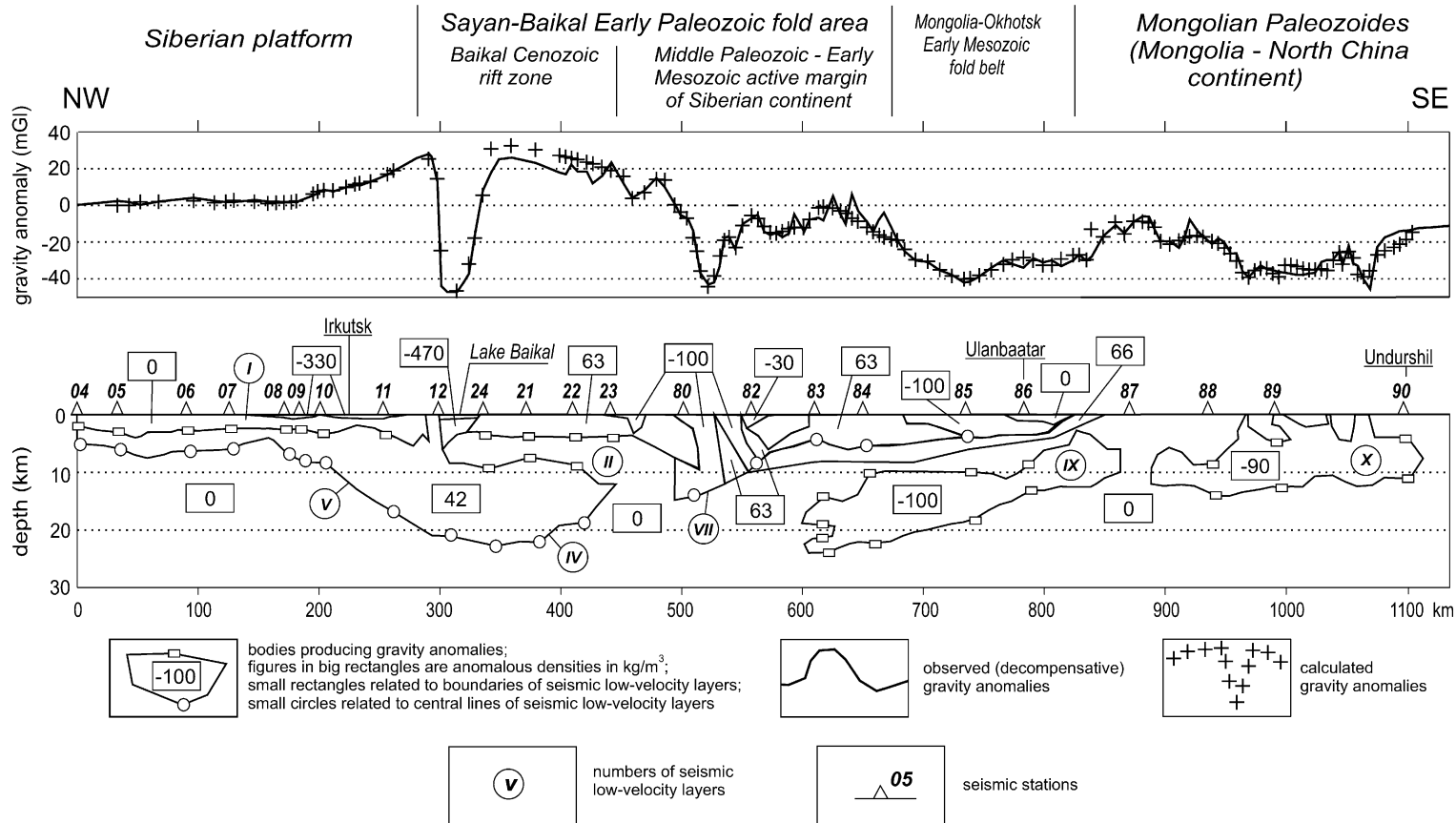
Fig. 10. Gravity model of the upper crust structure along the profile.

with the median lines or with the boundaries of the seismic low-velocity layers. For instance, the huge lens of Precambrian metamorphic rocks (Sharyzhalgay complex), bounded below by the median lines of the seismic layers IV and V and above by the layers I and II, has an average anomalous density of 42 kg/m^3 (Fig. 10). This complex corresponds to an ancient accretion wedge at the edge of the Archean Siberian craton (see below). The sheet above layer II has an average anomalous density of 63 kg/m^3. This sheet is composed of Early Paleozoic island arc complexes intruded by Late Paleozoic granites. We incorporated these granitic bodies in the gravity model using their exposures and anomalous densities (Zorin et al., 1994). The lower boundaries of granitic bodies between the stations 80 and 87 coincide with median line of the seismic layer VII (Fig. 10). As it will be shown below, this corresponds to a large-scale thrust.

Low-velocity zones IX and X (Fig. 10), based on their anomalous densities, correspond to large granitic bodies which have been previously proposed on the basis of gravity analysis and geological data (Zorin et al., 1994).

5.3. Geological interpretation

On the basis of the receiver function data and previous geological (Zorin et al., 1994) and gravity (see Section 5.2) data, we have constructed a combined cross-section of the Earth's crust along the seismic profile (Fig. 11). In this section, we attempt to give a geological interpretation for each identified low-velocity layer.

The extensive top low-velocity layer can be identified as the sedimentary Late Proterozoic and Lower Paleozoic cover only within the Siberian platform, where thickness of this layer is 2–3 km (Figs. 9 and 11)1991). There is no widespread sedimentary cover within the Eastern Siberian and Mongolian fold areas, where thickness of the uppermost low-velocity layer is 1–1.5 km (see Fig. 1). Existence of the layer in these mountain areas can be attributed to reduction of seismic velocity by deep weathering.

According to analysis of the thickness and the facies of both Late Proterozoic (Riphean) and Lower Paleozoic sedimentary strata (Mandelbaum, 1959; Zamaraev, 1967), the cover of the platform accumulated over an area that extended southeastward, far

beyond the present limits of the marginal (Baikal) uplift of the platform basement. This uplift developed only in the Late Ordovician–Silurian, during the collision of the Siberian platform with Vendian–Ordovician island arcs. The island arc seria and the Precambrian blocks, which formed the cores of some islands, overthrust the southern margin of the platform along the Sayan–Baikal suture (Zorin et al., 1993, 1994, 1995). Thus, it is possible that low-velocity layer II corresponds to the continuation of sedimentary cover of the platform beneath the allochthon.

Results from a seismic refraction survey (Krylov et al., 1999) along the axis of southern Lake Baikal suggest that the thickness of Cenozoic rift sediments reaches 5–6 km in the rift basin, but the depth of crystalline basement with a P-wave velocity of 5.9–6.2 km/s varies from 8 to 14 km. The intermediate layer with a P-waves velocity of 4.6–5.2 km/s and with a thickness of 3–8 km exists between the bottom of Cenozoic sediments and crystalline basement (Krylov et al., 1999).

The intermediate layer beneath the Baikal Rift Basin and above low-velocity layer II southeastward from the basin are situated at approximately the same depth. The P-wave velocity in the intermediate layer is 4.6–5.2 km/s, and the S-wave velocity in the layer II is 3.2–3.4 km/s. These values are close to the seismic velocities in the sedimentary cover of the Siberian platform (Pusyrev, 1993). Based on these data, we suggest that the intermediate layer beneath the Lake Baikal and above low-velocity layer II corresponds to an extension of the sedimentary cover of the Siberian platform. From the extension of the thickened part of the layer II (Fig. 11), the platform cover can be traced beneath the allochthon to the station 23, i.e., to a distance of about 125 km from southeastern edge of its exposed part. Early Paleozoic thrusts could have been renewed during later compression up to the Late Jurassic (Sizykh and Lobanov, 1994; Zorin, 1999).

With Late Cenozoic extension, some of the Early Paleozoic thrusts transformed into listric normal faults. Such reverse movement of the ancient allochthon led to the partial exhumation of the platform cover in the South Baikal region. As a result, Late Cenozoic sediments were deposited on the sedimentary cover of the Siberian platform in the axial and northwestern part of the rift basin, while in the southeastern part of the basin, the sediments were

NW

Siberian platform

Sayan-Baikal Early Paleozoic fold area

Baikal Cenozoic rift zone

Middle Paleozoic - Early Mesozoic active margin of Siberian continent

Mongolia-Okhotsk Early Mesozoic fold belt

Mongolian Paleozoides (Mongolia - North China continent)

SE

Irkutsk

Lake Baikal

Ulanbaatar

Undurshil

04 05 06 07 08 09 10 11 12 24 21 22 23 80 82 83 84 85 86 87 88 89 90

depth (km)

Sharyzhalgay suture

Mongolia-Okhotsk suture

Sayan-Baikal suture

Cenozoic sediments in Baikal rift basin

Early-Middle Jurassic continental sedimentary series

Late Paleozoic volcanics of Siberian active continental margin

Late Paleozoic granites of Siberian active continental margin

Middle-Late Paleozoic subduction-accretion wedge at active margin of Siberia

Vendian- Early Paleozoic island-arcs collided with Siberia at the Late Ordovician - Silurian

Late Proterozoic - Early Paleozoic cover of Siberian platform

Archean (?) - Early Proterozoic crustal block united Siberian platform at the Early Proterozoic

Early Proterozoic (Sharyzhalgay) metamorphic complex

Archean core of the Siberian platform

Paleozoic granites of Mongolia - North China continent

Early Paleozoic island-arc complex related to Mongolia - North China continent

Mongolia - North China continent (collage of Precambrian blocks and Paleozoic island-arcs)

main thrusts associated with suture zones

secondary thrusts

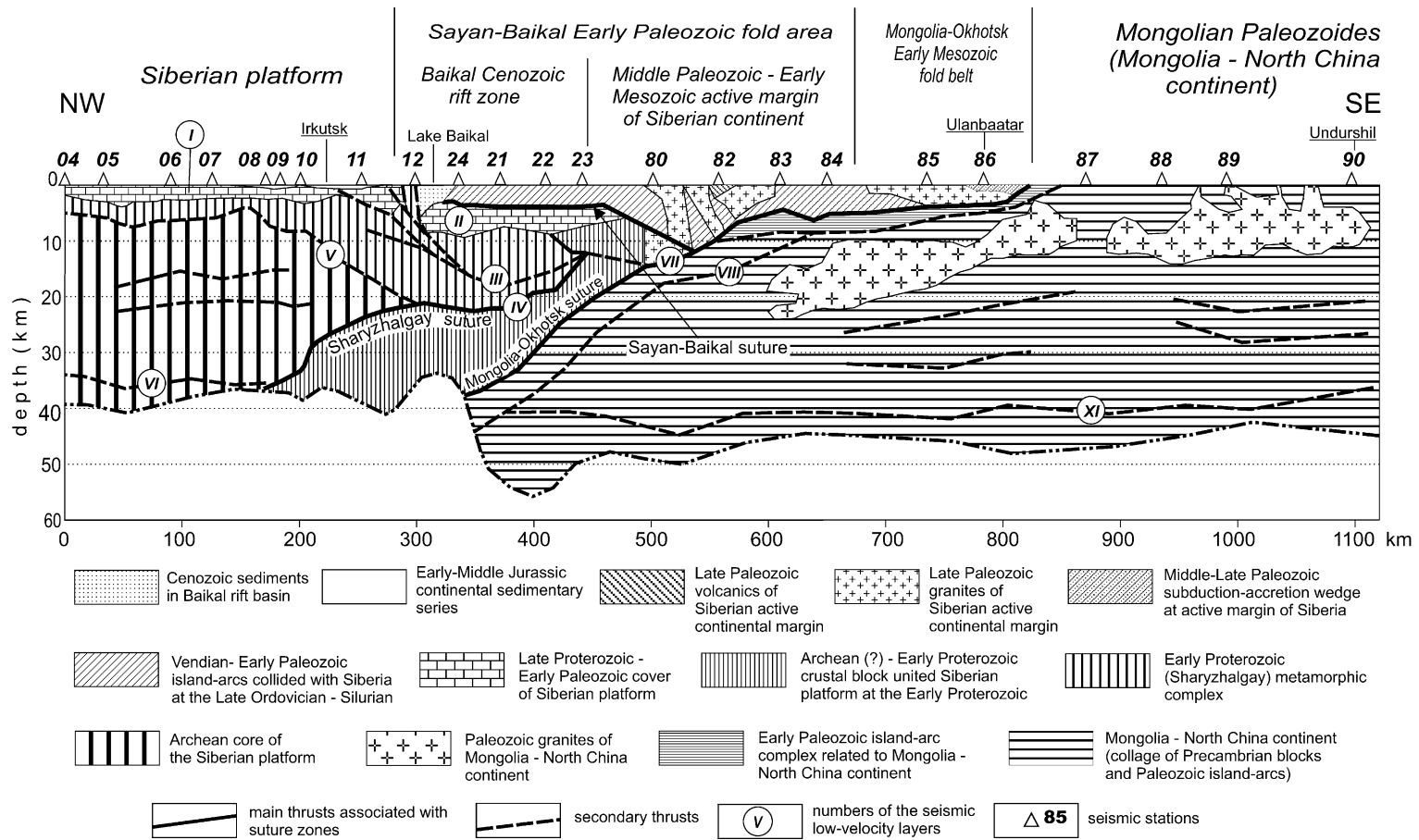V numbers of the seismic low-velocity layers

△ 85 seismic stations

Fig. 11. Cross-section of the Earth's crust constructed on the basis of combined interpretation seismic, gravity, and geological data. Geological and gravity data are taken from Zorin et al. (1994) and Zorin (1999).

deposited on allochthonous rocks (Fig. 11). It should be noted that transformation of the Early Paleozoic thrust into the Late Cenozoic listric faults has been proposed earlier on the basis of geological and some geophysical data (Logathcev and Zorin, 1992; Bulgatov, 1999).

Layer III (Fig. 9), which was also detected by DSS (Krylov et al., 1981; Pusyrev, 1993), is assumed to correspond to a tectonite zone related to an Early Paleozoic thrust of second order in the basement of the platform (Fig. 11). This thrust was probably rejuvenated by Cenozoic movements of a listric character and is situated at a depth favorable for rock dehydration under the present thermal conditions in the Baikal rift zone.

Penetration of layer IV across the entire crust allows us to assume that this layer is associated with a large-scale thrust, which is probably related to a relict zone of subduction under the ancient core of the Siberian platform. Based on geological data, a subduction zone with such an orientation existed here in the Early Proterozoic when magmatic phenomena typical of active continental margins of the Andean type developed on the marginal part of the platform (Zonnenshain et al., 1990). We propose that this thrust corresponds to the suture zone (we call it Sharyzhalgay suture according to the name of the Precambrian rock complex which is bordered by this suture from southeast). The rocks related to the Sharyzhalgay complex (turbidites with lenses of carbonates and dismembered ophiolites) were metamorphosed in the Early Proterozoic under collisional conditions (Hopgood and Bowes, 1990; Aftalion et al., 1991). The rock composition shows that the Sharyzhalgay complex corresponds to an accretionary wedge along the ancient margin of the Siberian platform. The Sharyzhalgay suture separates the Archean core of the Siberian platform and this accreted wedge from a crustal block which collided with the platform in the Early Proterozoic. This block is probably composed mainly of Archean and Early Proterozoic rocks (Fig. 11). Although we cannot distinguish any additional discontinuities within this block, there exists a possibility that the upper part of this block also includes Late Proterozoic (Riphean) arc island complexes that accreted to the platform in pre-Vendian time (Zorin et al., 1995).

The southeastward dipping layer V is distinguished beneath the platform and probably also corresponds to an ancient (Early Proterozoic) thrust. Together with the southeastern part of the layer IV, this layer bounds below a huge lens-like body formed by the Sharyzhalgay complex of metamorphic rocks of elevated density (Fig. 10). This body is exposed on the northwestern side of the Lake Baikal and, according to geophysical data, extends beneath the Sayan–Baikal fold area to the vicinity of the station 23 (Figs. 9–11).

The two unnumbered sub-horizontal low-velocity layers in the middle of the crust of the Siberian platform are interpreted as mylonite zones related to Precambrian low-angle thrusts (Fig. 11). Layer VI in the lower crust, near the Moho, may correspond to a mylonite zone formed by crustal sliding relative to the mantle. Such sliding, caused by a difference between the mechanical properties of the crust and the mantle, could take place during collisions (Molnar, 1989).

The location, where layer VII approaches the Earth's surface, is close to the Mongolia–Okhotsk suture zone, along which the Mongolia–North China continent accreted to the Siberian continent at the Early/Middle Jurassic boundary (Zorin et al., 1994; Zorin, 1999). It should be noted that the crust thickens abruptly southeastward of the location where the layer VII reaches the Moho (Figs. 9 and 11). It allows us to suggest that layer VII corresponds to a thick mylonite zone, related to the Mongolia–Okhotsk suture zone (Fig. 11), along which the active margin of Siberia overthrust the passive margin of the Mongolia–North China continent (Zorin et al., 1995; Zorin, 1999).

Low-velocity layer VIII (Figs. 9 and 10) may correspond to a Paleozoic thrust inside the Mongolia–North China continent which is a collage of Precambrian continental blocks and Paleozoic island arcs (Zorin et al., 1993, 1994, 1995). The dip of this layer correlates with orientation of subduction zone beneath the island arc which existed in the Early Paleozoic near the northern margin of this continent (Zorin et al., 1994).

The thick low-velocity zones IX and X within the Mongolian Paleozoids (Figs. 9 and 11) evidently correspond to large granitic bodies hosted by metamorphic strata of the upper part of the crust. As mentioned above, this proposal is in agreement with gravity data (Fig. 10): density deficits of these bodies are typical for granites (Zorin et al., 1994).

Four inextensive (unnumbered) low-velocity layers in the middle crust of the Mongolia–North China

continent (Figs. 8 and 10) probably mark low-angle thrusts in the Precambrian part of the crust. The interrupted low-velocity layer XI near the Moho (Fig. 9), as well as aforementioned layer VI, may correspond to mylonite zones formed by the sliding of the crust relative to the mantle during collisions.

6. Discussion and conclusions

Numerical modeling shows that the receiver function method can detect low-velocity layers in the Earth's crust if the thickness of these layers is no less than three vertical steps of the seismic model. These layers are identified by formal inversion of the receiver functions although seismic signals related to the boundaries of these layers cannot be visually determined directly from waveforms because of mutual superposition of the phases. This method requires a good initial approximation (starting model) to obtain reliable results. The starting S-waves velocity model used was based on the averaged DSS velocities for the Sayan–Baikal mountain region (Pusyrev, 1993). Such a starting model is a rather strong constraint on results of inversion, and consequently allows us to propose that the low-velocity layers are real rather than artifacts.

Most of the low-velocity layers (IV, V, VI, VII, VIII, XI, and several unnumbered ones) are suggested to correspond to thick mylonite zones related to the low-angle thrusts. The mylonite zones possess great seismic anisotropy with a minimum seismic velocity orthogonal to their foliations, and they behave as the low-velocity layers only for waves with rays close to that direction. Therefore, the receiver function method, which uses waves with the sub-vertical rays, is an appropriate tool to study the thick mylonite zones related to sub-horizontal thrusts. Some low-velocity layers may reflect sediment strata overthrust by the crystalline rock nappes (layer II) or can be associated with the granitic bodies (layers IX and X).

It should be noted that dip direction and large-scale character of the main thrusts have been proposed earlier on the basis of geological data (Zorin et al., 1994, Sizykh and Lobanov, 1994; Zorin, 1999, Bulgatov, 1999). These data were used as additional evidence for correlation of the low-velocity layers suggested to correspond to these thrusts (layers IV,

VII, VIII, and upper boundary of the layer II). We believe that such combined interpretation supported by the gravity model gives additional information on the deep geometry of these thrusts and on their horizontal extent across the strike.

We should note that in general, the extent of the mylonite zones on the cross-sections can significantly exceed displacement along the thrust. This concerns second-order thrusts (Fig. 11). It is not acceptable for the first-order thrusts corresponding to the suture zones separating the crustal blocks united (according to geological data) during collisions. In the latter case, the extent of the tectonite zones across the strike must reflect the overthrusting value. This parameter for the Sharyzhalgay suture is estimated as 250 km, for Sayan–Baikal one, it is not less than 250 km, and for Mongolo–Okhotsk suture, it is up to 450 km (Fig. 11). The given figures do not look shocking if compared to assumed underthrusting value of India beneath southern Eurasia with the formation of Tibetan Plateau as a result of doubling of the crust thickness after later (Oligocene) collision. This value is estimated as 1000 km (Ni and Barazangi, 1983).

In the Baikal rift zone, some of the Early Paleozoic thrusts transformed into listric faults during Late Cenozoic extension. As a result of extensional tectonics, the Cenozoic sediments in northwestern and axial part of the Baikal Basin were deposited on exhumed sedimentary cover of the Siberian platform, while on southeastern side of the basin, they were deposited on crystalline rocks of the Early Paleozoic allochthon.

In spite of the compatible picture which we propose based on combined interpretation of the seismic, gravity, and geological data, there could be certain doubts about its validity. We could use only the records of short-period seismographs. It would be better to use broadband records. To correlate some seismic low-velocity layers between the stations, we used geological data, i.e., this correlation was not independent. Moreover, it is possible that some weakly expressed low-velocity layers are artifacts. Therefore, some of interpretations could be ambiguous. It would be desirable to check the existence of the presumed thrusts and to map precisely their geometry by multichannel seismic profiling. It is expedient to perform this profiling first of all in the southeastern vicinity of the Lake Baikal, where the crystalline rocks are assumed to

overthrust the oil and gas containing sedimentary cover of the Siberian platform.

References

Aftalion, M., Bibikova, E.V., Bowes, D.R., Hopgood, A.M., Perchuk, L.L., 1991. Timing of Early Proterozoic collisional and extensional events in the granulite–gneiss–charnockite–granite complex, Lake Baikal, USSR: a U–Pb, Rb–Sr, and Sm–Nd isotopic study. Journal of Geology 99, 851–861.

Ammon, C.J., Randall, G., Zandt, G., 1990. On the non-uniqueness of receiver function inversion. Journal of Geophysical Research 95, 15303–15318.

Argutina, T.A., Bulavko, L.F., Bulin, N.K., Yudborovsky, I.Kh., 1974. Deep-seated geological structure of the Trans-Baikal region (in Russian). Sovetskaya Geologiya 11, 103–117.

Birch, F., 1961. The velocity of compressional waves in rocks to 10 kilobars, Part II. Journal of Geophysical Research 66, 2199–2224.

Bulgatov, A.N., 1999. Probable tectonic nature of Pre-Cenozoic sediment complex in southern basin of the Lake Baikal. Russian Geology and Geophysics 40 (10), 1511–1516.

Christensen, N.I., 1965. Compressional wave velocity in metamorphic rocks at pressures to 10 kilobars. Journal of Geophysical Research 70, 6147–6164.

Cordell, L., Zorin, Yu.A., Keller, G.R., 1991. The decompensative gravity anomaly and deep structure of the region of Rio Grande rift. Journal of Geophysical Research 96, 6557–6558.

Cordell, L., Phylipps, J.D., Godson, R.H., 1992. US Geological Survey Potential-Field Geophysical Software, Version 2.0, Open-File Report. US Geological Survey, Federal Center, Denver, 125 pp.

Gao, Sh., Davis, P.M., Liu, H., Slack, P.D., Zorin, Yu.A., Mordvinova, V.V., Kozhevnikov, V.M., Meyer, R.P., 1994. Seismic anisotropy and mantle flow beneath the Baikal rift zone. Nature 371, 149–151.

Haskell, N.A., 1962. Crustal reflection of plane P and SV waves. Journal of Geophysical Research 67, 4751–4767.

Hathcinson, D.R., Golmshtok, A.J., Zonenshain, L.P., Moore, T.C., Scholz, C.A., Klitgord, K.D., 1992. Depositional and tectonic framework of the rift basin of Lake Baikal from multichannel seismic data. Geology 20, 589–592.

Hopgood, A.M., Bowes, D.R., 1990. Contrasting structural features in the granulite–gneiss–charnockite–granite complex, Lake Baikal, U.S.S.R.: evidence for diverse geotectonic regimes in early Proterozoic times. Tectonophysics 174, 279–299.

Kind, R., Kosarev, G.L., Petersen, N.V., 1999. Receiver functions at the stations of the German Regional Seismic Network (GRSN). Geophysical Journal International 121, 191–202.

Krylov, S.V., Mandelbaum, M.M., Mishen'kin, B.P., Mishen'kina, Z.P., Petric, G.V., Seleznev, V.C., 1981. The Interior of Baikal from Seismic Data (in Russian). Nauka, Novosibirsk, 105 pp.

Krylov, S.V., Seleznev, V.S., Soloviev, V.M., Petric, G.V., Sheludko, I.F., 1999. Study of the Baikal rift basin by the seismic tomography method from refracted waves (in Russian). Doklady Rossijskoj Akademii Nauk 345 (5), 647–677.

Kurita, T., 1947. Upper mantle structure in the central United States from P- and S-wave spectra. Physics of the Earth and Planetary Interiors 8, 177–201.

Langston, C.A., 1979. Structure under Mount Rainier, Washington, inferred from teleseismic body waves. Journal of Geophysical Research 84, 4749–4762.

Logatchev, N.A., Zorin, Yu.A., 1992. Baikal rift zone: structure and geodynamics. Tectonophysics 208, 273–286.

Mandelbaum, M.M., 1959. Tectonics of Selenga depression and the problem of the Baikal oil (in Russian). In: Mineev, I.K. (Ed.), Materialy po Geologii i Poleznym Iskopaemym Vostochnoy Sibiri. Geologicheskoye Upravlenie, Irkutsk, pp. 89–97.

Molnar, P., 1989. The geological evolution of the Tibetan Plateau. American Scientist 77, 350–360.

Mordvinova, V.V., 1988. Spectral ratio of seismic oscillations and the lithosphere thickness in the southern regions of Siberia (in Russian). Fizika Zemli 5, 12–20.

Mordvinova, V.V., Zorin, Yu.A., Gao, Sh., Davis, P., 1995. The estimations of the thickness of the Earth's crust on the profile Irkutsk–Ulanbaator–Undurshill from the spectral ratio of the seismic waves (in Russian). Fizika Zemli 9, 35–42.

Ni, J., Barazangi, M., 1983. High-frequency seismic wave propagation beneath the Indian Shield, Himalayan arc, Tibetan Plateau, and surrounding regions: high uppermost mantle velocities and efficient S_n propagation beneath Tibet. Geophysical Journal of the Royal Astronomical Society 72, 665–689.

Petersen, L.P., Vinnik, L.P., 1991. Distinguishing of the crustal converted waves as the problem of multichannel filtration (in Russian). Fizika Zemli 4, 37–44.

Popov, A.M., 1989. Results of deep MT studies in light of data of other geophysical methods in the Baikal region (in Russian). Fizika Zemli 8, 31–37.

Pusyrev, N.N. (Ed.), 1993. Detailed Seismic Studies of the Lithosphere by P- and S-waves (in Russian). Nauka, Novosibirsk, 199 pp.

Rabbel, W., 1994. Seismic anisotropy at the Continental Deep Drilling Site (Germany). Tectonophysics 232, 329–342.

Sizykh, V.I., Lobanov, M.P., 1994. Thrust–nappe control of the oil and gas deposits of the south of the Siberian platform (in Russian). Doklady Rossijskoj Akademii Nauk 335 (5), 621–625.

Tikhonov, A.N., Arsenin, V.Ya., 1979. The Solution Methods of the Ill-posed Problems (in Russian). Nauka, Moscow, 288 pp.

Vinnik, L.P., Kosarev, G.L., Makeeva, L.I., 1988. Determination of the Earth's crust structure from the forms of P-wave oscillations (in Russian). In: Neresov, I.L. (Ed.), Structure and Dynamics of the Lithosphere from Seismic Data. Nauka, Moscow, pp. 5–18.

Zamaraev, S.M., 1967. Marginal Structure of the Southern Part of the Siberian Platform (in Russian). Nauka, Moscow, 248 pp.

Zonenshain, L.P., Kuzmin, M.I., Natapov, L.M., 1990. Geology of the USSR: plate tectonic synthesis. Am. Geophys. Union Geodyn. Ser., Washington, DC, vol. 21, 242 pp.

Zorin, Yu.A., 1999. Geodynamics of the western part of the Mongolia–Okhotsk collisional belt, Trans-Baikal region (Russia) and Mongolia. Tectonophysics 306, 33–56.

Zorin, Yu.A., Pismenny, B.M., Novoselova, M.R., Turutanov, E.Kh., 1985. Decompensative gravity anomalies (in Russian). Geologia i Geofizika 8, 104–108.

Zorin, Yu.A., Belichenko, V.G., Turutanov, E.Kh., Kozhevnikov, V.M., Ruzhentsev, S.V., Dergunov, A.B., Filippova, I.B., Tomurtogoo, O., Arvisbaatar, N., Baysgalan, Ts., Biambaa, Ch., Khosbayar, P., 1993. The South Siberia–Central Mongolia transect. Tectonophysics 225, 361–378.

Zorin, Yu.A., Belichenko, V.G., Turutanov, E.Kh., Mordvinova, V.V., Kozhevnikov, V.M., Khozbayar, P., Tumurtogoo, O., Arvisbaatar, N., Gao, Sh., Davis, P., 1994. The Baikal–Mongolian transect (in Russian). Geologia i Geofizika 7–8, 94–110.

Zorin, Yu.A., Belichenko, V.G., Turutanov, E.Kh., Mazukabzov, A.M., Sklyarov, E.V., Mordvinova, V.V., 1995. The East Siberia transect. International Geology Review 37 (2), 154–175.

Zorin, Yu.A., Zorina, L.D., Spiridonov, A.M., Rutshtein, I.G., 2001. Geodynamic setting of gold deposits in the Eastern and Central Trans-Baikal. Ore Geology Reviews 17 (4), 215–232.